

Tyrosine-Z in Oxygen-Evolving Photosystem II: A Hydrogen-Bonded Tyrosinate[†]Michael Haumann,[‡] Armen Mulikidjanian,^{‡,§} and Wolfgang Junge^{*,‡}

Abt. Biophysik, FB. Biologie/Chemie, Universität Osnabrück, D-49069 Osnabrück, Germany, and A.N. Belozersky Institute of Physico-Chemical Biology, Moscow State University, Moscow 118899, Russia

Received June 30, 1998; Revised Manuscript Received September 22, 1998

ABSTRACT: In oxygen-evolving photosystem II (PSII), a tyrosine residue, D1Tyr161 (Y_Z), serves as the intermediate electron carrier between the catalytic Mn cluster and the photochemically active chlorophyll moiety P_{680} . A more direct catalytic role of Y_Z , as a hydrogen abstractor from bound water, has been postulated. That Y_Z^{ox} appears as a neutral (i.e. deprotonated) radical, Y_Z^{\bullet} , in EPR studies is compatible with this notion. Data based on electrochromic absorption transients, however, are conflicting because they indicate that the phenolic proton remains on or near to Y_Z^{ox} . In Mn-depleted PSII the electron transfer between Y_Z and P_{680}^+ can be almost as fast as in oxygen-evolving material, however, only at alkaline pH. With an apparent pK of about 7 the fast reaction is suppressed and converted into an about 100-fold slower one which dominates at acid pH. In the present work we investigated the optical difference spectra attributable to the transition $Y_Z \rightarrow Y_Z^{ox}$ as function of the pH. We scanned the UV and VIS range and used Mn-depleted PSII core particles and also oxygen-evolving ones. Comparing these spectra with published in vitro and in vivo spectra of phenolic compounds, we arrived at the following conclusions: In oxygen-evolving PSII Y_Z resembles a *hydrogen-bonded tyrosinate*, $Y_Z^{(-)} \cdots H^{(+)} \cdots B$. The phenolic proton is shifted toward a base B already in the reduced state and even more so in the oxidized state. The retention of the phenolic proton in a hydrogen-bonded network gives rise to a positive net charge in the immediate vicinity of the neutral radical Y_Z^{\bullet} . It may be favorable both for the very rapid reduction by Y_Z of P_{680}^+ and for electron (not hydrogen) abstraction by Y_Z^{\bullet} from the Mn–water cluster.

Photosystem II (PSII)¹ produces molecular oxygen from water. It is located in photosynthetic membranes of plants and cyanobacteria. The inner core of PSII is a heterodimer of the D1D2 subunits which show homology with the L and M subunits of the purple bacterial RC (1). The primary electron donor of PSII, P_{680} , is located close to the luminal side of the membrane. The absorption of a quantum of light drives the charge separation between P_{680} and the quinone acceptor at the stromal side (2). The very high redox potential of P_{680}^+ drives water oxidation. It is a four-stepped process with at least four increasingly oxidized, metastable states S_0 to S_3 , plus a transient state S_4 that decays in milliseconds into S_0 under release of O_2 . P_{680}^+ is reduced (in nanoseconds) by a redox-active tyrosine residue, Y_Z (D1Tyr161 (3, 4)). Y_Z^{ox} is, in turn, reduced in microseconds by the oxygen-evolving complex (OEC). The structure and exact location of the OEC is still ill-defined. It is formed by four manganese

atoms (5, 6), possibly another redox cofactor, X (7–9), plus at least one Cl^- ion (10) and one Ca^{2+} (11, 12) ion. These cofactors serve various functions during water oxidation: The Mn cluster stores at least two of the oxidizing equivalents (namely on transitions $S_0 \Rightarrow S_1$ and $S_1 \Rightarrow S_2$ of the catalytic cycle) and may bind the reactive water molecules (5). It is proposed that the cofactor X is both oxidized and deprotonated on $S_2 \Rightarrow S_3$ (8, 9) and that the two ions adjust the redox potentials of the other compounds (8, 13).

Tyrosine Y_Z probably occupies a position on subunit D1 relative to P_{680} which is similar to the one of LArg135 or MHis162 in the reaction center of *Rhodospseudomonas viridis* (1, 14, 15). This has been inferred from the distance estimates of about 12 Å to P_{680} (15, 79–81) and a projection of about 4 Å on the membrane normal according to the relative electrogenicity of electron transfer between Y_Z and P_{680}^+ (16, 17). The function of tyrosine Y_Z is under debate. It has been proposed that Y_Z not only acts as an electron transmitter between the OEC (Mn_4X) and P_{680}^+ , but participates more directly in water oxidation. The neutral radical Y_Z^{ox} , formed by electron abstraction, was suggested to pick up a hydrogen atom from bound water after its deprotonation into the bulk (18–21). This concept has been mainly based on three sets of data and interpretations: (1) Y_Z^{ox} is a neutral radical (22). (2) The distance between Y_Z^{ox} and a second paramagnetic species is as low as <5 Å (23). (3) The oxidation of Y_Z causes proton release into the bulk (9, 25–28). Items 2 and 3 are highly debatable. The short distance estimates were obtained with centers which were depleted of Ca^{2+} so that oxygen evolution was impaired and electron transfer from

[†] Financial support by the Deutsche Forschungsgemeinschaft (Grant SFB171/A2, Mu-1258/1), the Fonds der Chemischen Industrie, the Land Niedersachsen, and INTAS (Grant 93-2852) is gratefully acknowledged.

* Corresponding author. Tel: ++49 541 969 2872. Fax: ++49 541 969 2870. E-mail: JUNGE@UOS.DE.

[‡] Universität Osnabrück.

[§] Moscow State University.

¹ Abbreviations: Bis-Tris, bis(2-hydroxyethyl)iminotris(hydroxymethyl)methane; β -DM, *n*-dodecyl- β -D-maltoside; DCBQ, 2,5-dichloro-*p*-benzoquinone; ENDOR, electron nuclear double resonance; EPR, electron paramagnetic resonance; Mes, 2-*N*-morpholinoethanesulfonic acid; Mn, manganese; NHE, normal hydrogen electrode; OEC, oxygen-evolving complex; PSII, photosystem II; P_{680} , primary donor in photosystem II; Phe, phenol; Q_A , primary electron acceptor quinone; RC, reaction center; X, chemically undefined cofactor; Y_Z , Y_D , tyrosines 161 on subunits D1 and D2 of PSII; UV, ultraviolet; VIS, visible.

Y_Z to P_{680}^+ was drastically slowed (from ns to μ s) (29). In their most recent paper, Britt and co-workers withdraw the small distances (24). The new estimates range now between 8.6 and 11.5 Å (24). Moreover, the other paramagnet may not be Mn but an organic radical (component X) (9, 30–32). The proton that appears in the medium upon formation of Y_Z^{ox} in oxygen-evolving PSII does not originate from the tyrosine itself but from peripheral amino acid groups which electrostatically interact with the charge residing transiently on Y_Z^{ox} and thereafter on the Mn cluster ((33), ref 34 for review).

If one supposes that a neutral tyrosine (p*K* in water about 10) is oxidized to a neutral radical, Y_Z^{ox} , as apparent from EPR data (22), the rate of its oxidation may be steered by the deprotonation of the phenolic side chain. However, the rate of the Y_Z oxidation by P_{680}^+ is fast (tens of nanoseconds) (115, 116), almost insensitive to H/D substitution (33, 35–37), and has a low activation barrier (37, 38), as characteristic for a pure electron-transfer event. Furthermore, the formation of Y_Z^{ox} is accompanied by a large and rapid electrochromic band shift of nearby pigments (15, 34, 39, 40).

We have recently studied the oxidation of Y_Z by P_{680}^+ and the accompanying protolytic and electrochromic transients both in oxygen-evolving and Mn-depleted preparations as function of the pH, isotopic substitution D/H, and temperature (37). In Mn-depleted centers we have found a drastic modulation of the reaction velocity by the pH with an apparent p*K* of about 7. Above pH 7 the reaction retains the same qualitative features as those observed in oxygen-evolving preparations, namely a fast rate (half-rise $\sim 1 \mu$ s), a small isotope effect, and a low activation barrier. At pH < 7, however, the properties of the reaction are dramatically altered: The relaxation time of Y_Z oxidation is about 100-fold longer, the activation energy increases from about 10 to 35 kJ mol⁻¹, the H/D isotopic ratio increases from 1.1 to about 2.5, and the extrusion of a proton into the bulk is detectable with the same rise time as the one of the electron transfer to P_{680}^+ . Moreover, the reaction $Y_Z \rightarrow Y_Z^{ox}$ is no longer accompanied by electrochromic band shifts in the blue spectral region. These results have been taken as evidence for the existence of partner bases to Y_Z . In oxygen-evolving centers they are ready to accept the phenolic proton of Y_Z^{ox} . The same holds in Mn-depleted centers at alkaline pH. If protonated, the oxidation of Y_Z by P_{680}^+ requires the prior release of the phenolic proton into the bulk. This was observed in Mn-depleted centers at acid pH. The electron transfer is then kinetically coupled to the proton transfer. With regard to the oxidation of Y_Z in oxygen-evolving centers we were unable to distinguish between two alternative models in our previous work (37): (1) The rapid and nearly activation-less oxidation of Y_ZH by P_{680}^+ may be accompanied by the non-rate-limiting shift of a proton within a preexisting hydrogen bond to a nearby base (B), yielding the species $Y_Z \cdots H^+ \cdots B$ as Y_Z^{ox} . (2) The hydroxylic proton may be absent already in the reduced form of Y_Z so that the anionic tyrosinate, Y_Z^- , is oxidized to yield the neutral radical Y_Z^\bullet .

In this work we compared optical transients upon the oxidoreduction of Y_Z in the UV, VIS, and near-IR spectral regions in oxygen-evolving and in Mn-depleted PSII core particles as function of the pH. We aimed at the spectral changes due to the oxidation of Y_Z proper and at the local

electrochromic band shifts of carotenoids and chlorophylls which are associated with the redox transients of Y_Z . Unlike EPR and ENDOR techniques that monitor only the paramagnetic radical species Y_Z^{ox} , flash spectrophotometry provides the difference spectrum $Y_Z^{ox} - Y_Z$. Hence it yields also information on the chemical nature of the EPR-invisible reduced state of Y_Z .

The shape of the UV difference spectrum of $Y_Z^{ox} - Y_Z$ was rather similar between oxygen-evolving centers at pH 5.5 and Mn-depleted ones at pH 9. In Mn-depleted centers the spectrum at acid pH (5.7) differed from the former two. In the UV it was broader and red shifted by about 10 nm, and in the blue and red regions local electrochromic effects were absent. The Y_Z spectra were compared with in vitro and in vivo spectra of phenolic compounds. The most likely interpretation of our data was as follows: In oxygen-evolving centers (and in Mn-depleted ones but only at alkaline pH) Y_Z is oxidized from a hydrogen-bonded tyrosinate ($Y_Z^{(-)} \cdots H^{(+)} \cdots B$) to a hydrogen-bonded radical ($Y_Z^\bullet \cdots H^+ \cdots B$) which is a positively charged entity.

MATERIALS AND METHODS

Oxygen-evolving PSII core particles were prepared from pea seedlings according to ref 41 with modifications as in ref 28 and stored at -80°C in 20 mM Bis-Tris/HCl, 400 mM sucrose, 20 mM MgCl₂, 5 mM CaCl₂, 10 mM MgSO₄, and 0.03% (w/v) β -DM at pH 6.3. These core particles lack the 17 and 23 kDa extrinsic proteins (28, 41). After thawing they were suspended at 10 μ M chlorophyll in 10 mM CaCl₂, 0.03% w/v β -DM, and 20 mM MES (pH 5.5, 5.7) or Tricine (pH 9).

Inactivation of core particles was achieved by gentle stirring of a suspension with 100 μ M of chlorophyll at pH 9 for 5 min at room temperature under dim light. The pH was readjusted for potentiometric and photometric measurements. After this treatment oxygen evolution under continuous illumination (not documented) was below 10% of a control. The pH 9 treated samples were indistinguishable from samples that were inactivated by the classical tris-wash treatment (42, 118) as apparent from transients of the reduction of P_{680}^+ at 820 nm (37). Accordingly, it was likely that they were depleted of manganese (37, 42–44). It should be noted that the rate of the reduction of P_{680}^+ in pH 9 and tris-treated samples differed from the one in calcium-depleted material. This will be outlined in a forthcoming publication (see ref 119).

Flash-spectrophotometry was performed with the basic setup described in ref 45. The measuring light from a CW tungsten lamp (Osram, $\lambda > 350$ nm) or a pulsed deuterium lamp (Cathodeon, $\lambda < 350$ nm) was passed through a monochromator (bandwidth 4 nm) and farther through the cuvette (optical path length 1 cm) to hit a photomultiplier which was shielded against the saturating exciting flashes (Xenon lamp, pulse duration 10 μ s) by appropriate broad-band filters. The monochromator was calibrated by narrow interference filters. For measurements in the UV, in the blue, and in the green spectral region samples were excited at > 610 nm; for measurements in the red samples were excited at 400–500 nm. For measurements in the red region the photomultiplier was placed at a distance of 50 cm from the cuvette to suppress transient chlorophyll fluorescence by

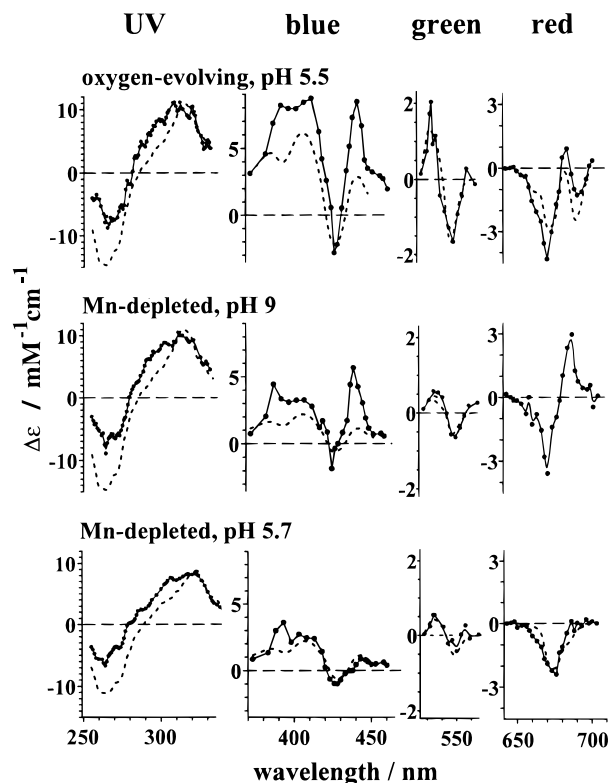


FIGURE 1: Flash-induced raw difference spectra (solid lines) from PSII core particles in the UV, blue, green, and red spectral regions. Spectra were recorded with material which was active in oxygen evolution at pH 5.5 (upper row) and with Mn-depleted centers at pH 9 (middle row) and 5.7 (bottom row). The respective extents (solid circles) were obtained as outlined under Materials and Methods. The spectra represent the average of 2–3 measurements. From the raw spectra (solid lines) the major contribution due to the oxidoreduction of Q_A and minor contributions from P_{680} and the Mn cluster were subtracted (dashed lines) to yield the corrected difference spectra $Y_Z^{ox} - Y_Z$ as shown in Figure 2. This correction was detailed in the text. Minor variations of the extents of the subtracted components did not abolish the differences between the corrected $Y_Z^{ox} - Y_Z$ spectra as shown in Figure 2.

spatial filtering. Transients were digitized (electrical bandwidth 3–30 kHz) and averaged (10–50 transients) on a Nicolet Pro30 recorder and stored on a MicroVax. The calibration of absorption transients in terms of $\Delta\epsilon$ was performed on the basis of 85 chlorophyll molecules per PSII in the core particles (28). Spectra were not corrected for (small) flattening effects.

RESULTS

Raw Absorption Difference Spectra and Their Deconvolution. Figure 1 shows the extents of absorption transients (solid circles) as taken at a given time delay (see below) after the firing of a flash of light in a series. The *top row* shows transients obtained with oxygen-evolving PSII core particles at pH 5.5. The two *lower rows* show transients obtained in Mn-depleted core particles at pH 9 (middle) and pH 5.7 (bottom).

The *difference spectra in the UV* are shown in the left column of Figure 1. With oxygen-evolving material at pH 5.5 (UV, solid circles) the extents at 20 μ s after the first flash which induced mainly transition $S_1 \rightarrow S_2$ of the OEC (28) were recorded. In the presence of 10 μ M DCBQ plus 30 μ M DCMU these transients reflected the formation of

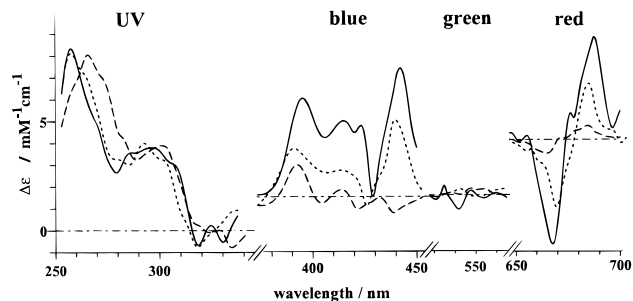


FIGURE 2: Corrected difference spectra of $Y_Z^{ox} - Y_Z$ in oxygen-evolving PSII core particles at pH 5.5 (solid line) and in Mn-depleted centers at pH 9 (dotted line) and pH 5.7 (dashed line) in the UV, blue, green, and red spectral regions. The precision of the spectra was within 1.5 units of the coordinate scale.

the couple $Q_A^- Y_Z^{ox}$. Y_Z^{ox} was reduced with a half-time of 85 μ s by the OEC upon transition $S_1 \rightarrow S_2$ (33), and Q_A^- recombined in seconds (46) with S_2 . With Mn-depleted material the extents at 1 ms after an exciting flash (repetition rate 0.1 Hz) were recorded with 10 μ M DCBQ and 30 μ M DCMU (Figure 1, UV, solid circles). These transients were again due to the formation of $Q_A^- Y_Z^{ox}$. Both species decayed slowly (half-times about 100 ms) by recombination (37, 47). Whereas the raw extents at pH 9 (Figure 1, UV, middle) were similar to the ones obtained with active centers (Figure 1, UV, top), they differed from the latter at pH 5.7 (Figure 1, UV, bottom). The oxidation of Y_Z alone causes only very small spectral changes in the region between 320 and 340 nm (47, 48). The respective extent in this region is therefore mainly attributable to $Q_A \rightarrow Q_A^-$. Several difference spectra of the latter reaction in the UV and blue spectral regions have been reported in the literature (see for example refs 4, 8, 49, 50, and 120). These spectra were all very similar although they have been obtained with different PSII preparations which were purified from different organisms. The Q_A/Q_A^- difference spectrum was further found to be pH independent (47). To remove the contribution of Q_A/Q_A^- from our UV spectra we normalized its difference spectrum (taken from Dekker et al. (49)) to the observed UV extents at around 325 nm (Figure 1, UV, dotted lines) and subtracted it from the former. The resulting differences from active centers and from inactive ones at pH 5.7 were scaled by factors of 1.2 to account for the amount of centers where Y_Z^{ox} has decayed after 20 μ s in the former case and for a proportion of about 20% of total P_{680} which stayed oxidized, P_{680}^+ , in equilibrium with Y_Z^{ox} (37). To correct for the spectral contribution of $P_{680} \rightarrow P_{680}^+$, we furthermore subtracted 20% of its difference spectrum as taken from Gerken et al. (50) from the data points at pH 5.7. In active centers (and also in inactive ones at pH 9) the equilibrium proportion of P_{680}^+ was negligible (37). We also subtracted another component, namely 20% of the difference spectrum $S_2 - S_1$ as taken from van Leeuwen et al. (51). The major contributions to our UV difference spectra were due to Y_Z^{ox}/Y_Z and Q_A^-/Q_A (see Figure 1). The subtraction of the latter contribution was reliable owing to its good reproducibility (see above). It should be noted that the differences between our deconvoluted difference spectra $Y_Z^{ox} - Y_Z$ were robust toward small changes of the subtracted contributions of Q_A^-/Q_A , P_{680}^+/P_{680} , and S_2/S_1 . The corrected difference spectra of $Y_Z^{ox} - Y_Z$ are shown in Figure 2 (UV) as a solid line (oxygen-evolving centers, pH 5.5), a dotted line (Mn-depleted

centers, pH 9), and a dashed line (Mn-depleted centers, pH 5.7).

Spectra in the Blue and Green Regions (Figure 1). With oxygen-evolving centers we recorded the extents of absorption transients at 20 μ s after a single exciting flash (repetition rate 0.03 Hz) in the presence of 10 μ M DCBQ and 30 μ M DCMU. In the blue spectral region (Figure 1, blue, top, solid circles) this spectrum reflected the formation of $Q_A^-Y_Z^{ox}$ (see above). With Mn-depleted centers we recorded the extents at 1 ms after a flash (repetition rate 0.1 Hz) with 100 μ M DCBQ and 1 mM hexacyanoferrate(III). This difference spectrum (Figure 1, blue column, solid circles; pH 9, middle; pH 5.7, bottom) mainly reflected the formation of Y_Z^{ox} because this species decayed in <100 ms whereas Q_A^- was mainly oxidized in less than 100 μ s by DCBQ/hexacyanoferrate (52). At pH 9 the raw extents were about halved with respect to the ones in oxygen-evolving centers. At pH 5.7 the observed transients were even much smaller. In the green spectral region (Figure 1, green) the negative charge on Q_A^- caused an electrochromic band shift around 550 nm (Figure 1, green, solid circles). It is probably attributable to the pheophytin of branch A (15, 47). We calibrated the contributions of Q_A^- to the spectra in the blue region on the basis of the electrochromic band shifts in the green (Figure 1, green, dotted lines). The scaled spectra of Q_A^- (taken from ref 47) are shown as dotted lines in the blue column of Figure 1. They were subtracted from the raw data. From the spectra from oxygen-evolving centers and Mn-depleted ones at pH 5.7 minor contributions of P_{680}^+ were subtracted as derived above (normalized at 430 nm, data taken from ref 50). The resulting differences from oxygen-evolving centers and Mn-depleted ones at pH 5.7 were further scaled by factors of 1.2 to account for the centers where Y_Z^{ox} was already rereduced after 20 μ s in the former, and for the equilibrium proportion of P_{680}^+ (see above) in the latter case. The resulting spectra $Y_Z^{ox} - Y_Z$ in the blue and green regions are shown in Figure 2 (solid lines, oxygen-evolving centers, pH 5.5; dotted lines, Mn-depleted centers, pH 9; dashed lines, Mn-depleted centers, pH 5.7).

Spectra in the Red Region (Figure 1). With oxygen-evolving material we recorded the extent at 1 ms after the third flash in a series with 50 μ M DCBQ. The samples were repetitively synchronized in state S_1 prior to the first flash by spacing the flash series by 20 s (repetitive dark-adaptation (28)). These extents (Figure 1, red column, top row, solid circles) were a superimposition of contributions from $Y_Z \rightarrow Y_Z^{ox}$, $Q_A \rightarrow Q_A^-$, and $P_{680} \rightarrow P_{680}^+$. Y_Z^{ox} decayed with a half-time of 4.6 ms upon $S_4 \rightarrow S_0$ (53), Q_A^- was reoxidized with a half-time of about 10 ms (52), and a small fraction of P_{680}^+ was reduced in milliseconds (37). With Mn-depleted material the extents at 1 ms after a flash (repetition rate 0.1 Hz) were recorded with 200 μ M DCBQ and 1 mM hexacyanoferrate(III). These extents (Figure 1, red column, solid circles; pH 9, middle; pH 5.7, bottom) were mainly due to Y_Z^{ox} which was stable for >100 ms (plus minor admixtures of transients from P_{680}^+ ; see below). Q_A^- was reoxidized in <100 μ s. From the red spectrum from oxygen-evolving centers the contribution of Q_A^- reduction was subtracted after normalization of its spectrum (taken from ref 15) at 690 nm where the changes from Y_Z^{ox} are negligible. The contributions of P_{680}^+ were also subtracted after normalization of the spectrum from ref 54 at 678 nm. The

sum of the subtracted components is shown as dotted line in Figure 1 (red column, top). The resulting difference was scaled by a factor of 2.5 to account for the amount of only 50% of centers in S_3 which reduced Y_Z^{ox} with a half-time of 4.6 ms (53) and for the portion of Y_Z^{ox} which has decayed after 1 ms. The spectrum of Mn-depleted centers at pH 9 was used without further correction. In Mn-depleted centers at pH 5.7 already the raw spectrum was strongly different from the former ones. The contribution of P_{680}^+ was subtracted (data taken from ref 54) after normalization at 678 nm (Figure 1, red, bottom, dotted line). The resulting spectra are again attributable to $Y_Z^{ox} - Y_Z$, and they are shown in Figure 2 (solid line, oxygen-evolving centers, pH 5.5; dotted line, Mn-depleted centers, pH 9; dashed line, Mn-depleted centers, pH 5.7). Again, the resulting differences attributable to $Y_Z^{ox} - Y_Z$ were robust toward small variations of the subtracted contributions from the other components.

Corrected Difference Spectra $Y_Z^{ox} - Y_Z$ in Oxygen-Evolving and Mn-Depleted PSII Core Particles. Figure 2 shows the deconvoluted difference spectra of $Y_Z^{ox} - Y_Z$ in oxygen-evolving centers at pH 5.5 (solid line) and in Mn-depleted centers at pH 9 (dotted line) and pH 5.7 (dashed line).

In the UV the spectra directly reflected the oxido reduction of tyrosine Y_Z . In this spectral region the data from oxygen-evolving material at pH 5.5 (solid line) and from Mn-depleted centers at pH 9 (dotted line) were alike (Figure 2). They conformed with published difference spectra as obtained with oxygen-evolving centers at pH 5.2 (121) and with Mn-depleted centers at more alkaline pH (pH 5.9 (4), pH 6 (56), pH 7.5 (48), pH 8.3 (47, 55, 120); see also ref 57 for a survey of these spectra). Contrastingly, the corrected difference spectrum of Mn-depleted centers at pH 5.7 (Figure 2, dashed line) clearly deviated from the former ones: The major peak was red shifted by about 10 nm. Around 300 nm the spectrum was somewhat broadened. A similar (although less pronounced) red shift has previously been observed at pH 5 with Mn-depleted centers (55).

In the blue spectral region the absorption transients were composed of electrochromic shifts of the Soret bands of the chlorophyll(s) of P_{680} , of pheophytin_A, and of at least one additional chlorophyll (15), in response to a charge on or near Y_Z^{ox} (see below and Discussion). These transients were superimposed by contributions from the oxido reduction of tyrosine itself, mainly around 400 nm (58). The largest extent at 443 nm, attributable to electrochromism, was observed with oxygen-evolving material (Figure 2, blue, solid line). Its difference spectrum was similar to previously reported ones (4, 40, 47, 48, 59, 60). With Mn-depleted centers at pH 9 the spectral shape was similar to the former ones; however, the extent was about halved (Figure 2, blue, dotted line). The diminution of electrochromism may be attributed to an increased local dielectric permittivity which halved the local electric field strength (16). Such an increase is plausible in view of a more open structure of PSII after removal of the Mn cluster. At pH 5.7 electrochromism was practically absent (Figure 2, blue, dashed line) in agreement with our earlier data (37) and only a small chemical contribution from Y_Z^{ox} itself remained around 400 nm (58).

Other authors have previously reported difference spectra of $Y_Z^{ox} - Y_Z$ in Mn-depleted PSII. Those obtained at a pH value around 6 units revealed electrochromic portions (4,

47, 56, 121), at first glance, at variance with our results. We have previously shown that the apparent pK with which the electrochromic effect in response to the formation of Y_Z^{ox} disappears depends on the preparation: It was 7 in the van Leeuwen/Bögershausen type of core particles as used in this work (and in ref 37 but 6 in a core preparation according to Ghanotakis/Lübbbers (37). This pK variation has been attributed to the influence of different detergents. It is conceivable that they alter the dielectric properties of the protein environment of Y_Z (37). The results in refs 4, 56, and 120 have been obtained with core particles from cyanobacteria which are more resistant to detergent treatment as obvious from measurements of proton release: Thylakoid-like oscillations of proton release were conserved in PSII from cyanobacteria in the presence of detergent but lost in preparations from plant material (122). We conclude that the apparent pK with which electrochromism due to Y_Z^{ox} disappears was ≤ 6 in the core particles from cyanobacteria as used in refs 4, 56, and 120. In PSII-enriched membranes as used in ref 47 a pK of ~ 6 has been shown to be coupled with the oxidation of Y_Z (60, 118), and electrochromism decreased at a pH below that pK (60), in accord with our results.

In the green spectral region (carotenoids) it was apparent that there were no electrochromic components attributable to Y_Z^{ox} itself. This served as a control for the correct subtraction of the contributions of Q_A^- from the blue and green spectra (see Figure 1 and Materials and Methods). The remains were negligible (Figure 2, green column).

In the red spectral region electrochromic shifts of the Q_y -transition bands of the inner pigments (chlorophylls, pheophytins) of PSII are observed (ref 15 and references therein). Active material (Figure 2, red column, solid line) yielded the largest, red-directed band shift. This band shift was the sum of contributions from at least three different pigments. That the band shifts were indeed electrochromic in nature and caused by a positive charge was apparent from a comparative analysis of transients upon the formation of Y_Z^{ox} , S_2 , and Q_A^- which could be simulated under the assumption of a reasonable geometry of the same set of pigments (15). In Mn-depleted centers at pH 9 (dotted line) the extent of the spectrum was again about halved. More importantly, it was nearly absent in Mn-depleted centers at pH 5.7 (dashed line). Under these conditions there was neither electrochromism in the red nor in the blue spectral region. It is straightforward to conclude that the transition $Y_Z \rightarrow Y_Z^{ox}$ was essentially electroneutral in Mn-depleted centers at pH 5.7.

Comparison of the UV Difference Spectra of Y_Z with Those of Phenolic Compounds. Variations of the difference spectra $Y_Z^{ox} - Y_Z$ may, in principle, result from a change in the spectrum of the reduced species, the oxidized one, or of both.

Figure 3A shows absolute spectra of some phenolic compounds from the literature. The overall shapes of these radical spectra are very similar. This indicates that the absorption is mainly due to the phenolic group. Open circles represent the neutral tyrosine radical (Tyr^\bullet) (data from ref 58) in water. Open squares represent the neutral phenol radicals (Phe^\bullet) as measured in water (data from ref 58), and open triangles measured in an aprotic medium, paraffin (data from ref 61). The spectrum in paraffin is shifted to the red by about 15 nm but otherwise similar to the one in water.

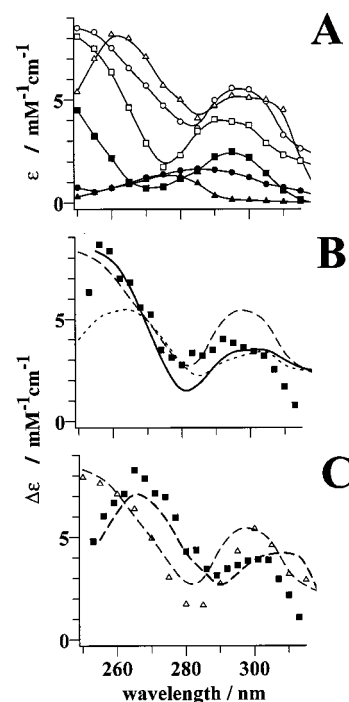


FIGURE 3: (A) Absolute radical spectra from tyrosine in water (open circles (58)), from phenol (58, 61) in water (open squares) and paraffin (open triangles), and spectra of reduced tyrosine at pH 7 ($TyrH$, solid triangles) and at pH 12 (Tyr^- , solid squares) in water. The solid circles show the spectrum of a hydrogen-bonded tyrosinate ($Tyr^{(-)\cdots H^{(+)}\cdot B}$) from calmodulin (63). (B) Comparison of the experimental difference spectrum $Y_Z^{ox} - Y_Z$ (squares) from oxygen-evolving PSII at pH 5.5 with calculated difference spectra from literature data: solid line, $Tyr_{H_2O}^\bullet - Tyr^{(-)\cdots H^{(+)}\cdot B}$; dashed line, $Tyr_{H_2O}^\bullet - TyrH$; dotted line, $Tyr_{H_2O}^\bullet - Tyr^-$. (C) Comparison of the experimental difference spectrum $Y_Z^{ox} - Y_Z$ (squares) from Mn-depleted PSII at pH 5.7 with the calculated difference spectrum $Phe_{paraffin}^\bullet - PheH$ (strong dashed line). The triangles represent the spectrum $Y_D^{ox} - Y_D$ from ref 56, and the thin dashed line the spectrum $Tyr_{H_2O}^\bullet - TyrH$ from Figure 3B.

The latter shift may be considered as the upper limit. Smaller shifts were observed in other aprotic solvents (61). The shift to the red in the aprotic medium is consistent with the absence of hydrogen-bonding to the radical as also apparent from model calculations (D. Cherepanov, personal communication). The spectra of tyrosine at pH 7 ($TyrH$, solid triangles) and of tyrosinate at pH 12 (Tyr^- , solid squares) in water (62) are also shown in Figure 3A. Spectra of the respective phenol or cresol species were very similar (not shown), which again indicates that the absorption is mainly due to the phenolic group. The overall absorption of the radicals (open symbols) is much higher than both of $TyrH$ and Tyr^- (Figure 3A). Recently, difference spectra of tyrosine radicals from pulse radiolysis experiments have been presented (57). These spectra were largely shifted (up to 40 nm) to red wavelengths when compared to other *in vitro* spectra in a large body of literature (58, 61, 69, 70) and to Y_Z in PSII (see Figure 3), and the extinction coefficients in the UV in ref 57 were smaller, about 50–75% of the values obtained for the oxidation of tyrosine *in vitro* (58, 61, 69, 70) and in PSII (see ref 57 and references therein). Furthermore, the contribution of the reduced state to the oxidized-minus-reduced spectra seemed to be much higher than in other *in vitro* and *in vivo* spectra (see above). The reasons for these discrepancies are still unknown. We

Table 1: Average Deviations $\Delta(\Delta\epsilon)$ between the Difference Spectra $Y_Z^{\text{ox}} - Y_Z$ from This Work and Calculated Model Difference Spectra of Phenolic Compounds [#]

PSII spectrum:	$Y_Z^{\text{ox}} - Y_Z$, O ₂ -evolving centers, pH 5.5	$Y_Z^{\text{ox}} - Y_Z$, Mn-depl. centers, pH 9	^b $Y_D^{\text{ox}} - Y_D$	$Y_Z^{\text{ox}} - Y_Z$, Mn-depl. centers, pH 5.7
model spectrum	average deviation, $\Delta(\Delta\epsilon)$			
$\text{Tyr}^*_{\text{H}_2\text{O}} - \text{Tyr}^{(-)\cdots\text{H}^{(+)}\cdot\text{B}}$	0.33 (0.26) ^a	0.41	0.28	>1.0
$\text{Tyr}^*_{\text{H}_2\text{O}} - \text{Tyr}^-$	0.48 (0.52) ^a	0.55	0.43	
$\text{Tyr}^*_{\text{H}_2\text{O}} - \text{TyrH}$	0.43 (0.39) ^a	0.54	0.22	
$\text{Phe}^*_{\text{paraffin}} - \text{Tyr}^{(-)\cdots\text{H}^{(+)}\cdot\text{B}}$	>1.0			0.64 (0.63) ^c
$\text{Phe}^*_{\text{paraffin}} - \text{Phe}^-$				0.94 (0.66) ^c
$\text{Phe}^*_{\text{paraffin}} - \text{PheH}$				0.44 (0.50) ^c

[#] For references for the model spectra see text. The average deviation was defined as $\Delta(\Delta\epsilon) = (\sum |i - x|)/n$ with i and x being the $\Delta\epsilon$ values of the $Y_Z^{\text{ox}} - Y_Z$ and the model spectrum at a given wavelength and n the number of data points. ^a Figures for the replacement of Tyr^{*} by Phe^{*}. ^b Data from ref 56. ^c Figures for the replacement of Phe^{*}_{paraffin} by Tyr^{*}_{H₂O} and shifting the latter spectrum by 10 nm to the red.

preferred to use the more consistent set of spectra from the elder literature (58, 61, 69, 70) for our simulations.

The absorption spectrum of TyrH in proteinaceous environments has been generally shown to be similar to the one in water (here not shown, see ref 63–66). In some proteins tyrosine residues with tyrosinate-like fluorescence spectra have been observed (63–65, 67, 68). Their action spectra have been interpreted as indicating hydrogen-bonded tyrosinates with the proton shifted to the bond acceptor rather than fully deprotonated tyrosinate residues (62). The position of the absorption peak of the *hydrogen-bonded tyrosinate* ($\text{Tyr}^{(-)\cdots\text{H}^{(+)}\cdot\text{B}}$) was found to be different from both TyrH and Tyr⁻. An example for such a spectrum is shown in Figure 3A with solid circles (data points from calmodulin (63)).

We aimed at a simulation of the experimental difference spectra from Y_Z in PSII by linear combinations of the in vitro radical and reduced state spectra. Figure 3B shows the difference spectrum of $Y_Z^{\text{ox}} - Y_Z$ as obtained in oxygen-evolving PSII in this work (squares). The calculated difference spectra of ($\text{Tyr}^*_{\text{H}_2\text{O}} - \text{TyrH}$) (dashed line) and ($\text{Tyr}^*_{\text{H}_2\text{O}} - \text{Tyr}^-$) (dotted line) approximate this spectrum rather poorly. As a quantitative criterion for the quality of the approximation we calculated the average deviations of the model spectra from the experimental data points. They are listed in Table 1. The lowest deviation was found (Table 1) if the calculated difference spectrum between the solvated tyrosine radical (e.g. obtained in aqueous solution) and the hydrogen-bonded tyrosinate ($\text{Tyr}^*_{\text{H}_2\text{O}} - \text{Tyr}^{(-)\cdots\text{H}^{(+)}\cdot\text{B}}$) was used (solid line). Replacing tyrosine by phenol in the model spectra gave comparable results (see Table 1).

The experimental difference spectrum of Y_Z at pH 5.7 in Mn-depleted PSII (Figure 3C, squares) was red shifted by about 10 nm with respect to the spectrum of oxygen-evolving centers (see Figure 3B). The spectrum of the nonsolvated phenol species in an aprotic medium (paraffin) was a fair approximation to our spectrum (–Mn, pH 5.7). The best approximation was given with the protonated phenol in the reduced state, e.g. by the calculated difference (phenol^{*}_{paraffin} – phenolH) (Figure 3C, strong dashed line, other simulations not shown; see Table 1 for the average deviations). Replacing Phe^{*}_{paraffin} by Tyr^{*}_{H₂O} and shifting the latter spectrum by 10 nm to the red gave comparable results (Table 1). Figure 3C

also shows the difference spectrum of Y_D (triangles) that has been reported by Diner et al. (56). This spectrum most closely resembles the calculated case ($\text{Tyr}^*_{\text{H}_2\text{O}} - \text{TyrH}$) (thin dashed line); the average deviation is lower than in the cases with tyrosinate or with the hydrogen-bonded tyrosinate in the reduced state (Table 1).

Summary of This Section. The comparison of the UV difference spectra of Y_Z in PSII with in vitro spectra of tyrosine and phenol indicated the following: In oxygen-evolving PSII core particles (and in Mn-depleted ones above pH 7) the reduced form of Y_Z resembles a hydrogen-bonded tyrosinate, $Y_Z^{(-)\cdots\text{H}^{(+)}\cdot\text{B}}$. The hydrogen bond is sustained in the oxidized form as compatible with EPR and ENDOR results (71–73). Although the radical Y_Z^{ox} itself is electro-neutral, the entity $Y_Z^{\text{ox}}\cdots\text{H}^+\cdot\text{B}$ is positively charged. This conforms with our data on electrochromism. The properties of Y_Z in Mn-depleted centers at pH < 7 are different: The reduced form of Y_Z is only weakly hydrogen bonded or not bonded at all ($Y_Z\text{H}$). For its reaction with P_{680}^+ to proceed, the phenolic proton has to be released into the bulk as in fact detected by using appropriate pH indicators (37). In this case, Y_Z^{ox} is electrically neutral. The situation is different for the second tyrosine, Y_D . Its reduced form ($Y_D\text{H}$) is weakly or not hydrogen bonded (Table 1) whereas the radical Y_D^{ox} is hydrogen bonded as shown by EPR and ENDOR (71–76).

DISCUSSION

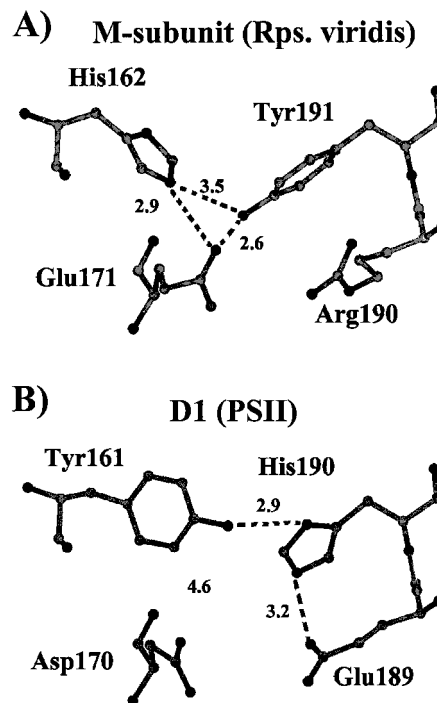
The charge separation in PSII is stabilized by a rapid secondary reaction between P_{680}^+ and Tyr161, Y_Z . It proceeds on the nanosecond time scale thereby preventing the charge recombination between P_{680}^+ with Q_A^- and deleterious side reactions with other components. What are the prerequisites for the rapid reduction of P_{680}^+ ? According to the Marcus theory (77) the rate of nonadiabatic electron transfer is determined by the edge-to-edge distance between donor and acceptor, the reorganization energy, and the standard redox potential difference of the reaction partners. For Y_Z and P_{680} the latter is reportedly smaller than or equal to 100 mV (4, 15, 78) (the equilibrium between $Y_Z\text{P}_{680}^+$ and $Y_Z^{\text{ox}}\text{P}_{680}$ is by more than 90% poised to the right). The center-to-center distance between P_{680} and Y_Z has been determined as ≥ 12 Å (15, 79–81) which corresponds to an edge-to-edge distance of ≥ 8 Å. The activation energy was very low, about 10 kJ mol⁻¹ (37, 38). Taking the gross kinetical ruler of Moser et al. (82) at face value and using the observed rate of electron transfer between Y_Z and P_{680}^+ , about 5×10^7 s⁻¹ in oxygen-evolving PSII (8, 37, 83–86), we calculated a reorganization energy of about 0.5 eV (123, 124). An even higher reorganization energy, 0.7 eV, has been obtained, for instance, for the electron transfer (in ~200 ps) from bacteriopheophytin to Q_A in the bacterial reaction center (see ref 82 and references therein). The latter figure is fully explained by the minor contribution to the reorganization energy of the large pheophytin molecule plus a major contribution of the smaller quinone ring (87). It is unnecessary to invoke contributions from proton movements to the reorganization energy of electron-transfer $Y_Z \rightarrow \text{P}_{680}^+$. As noted in the Introduction, the data on the operation of Y_Z in oxygen-evolving centers (33, 37, 40) are compatible (37) with either of two alternative models: (1) with a prompt displacement of the hydroxyl proton into a hydrogen bond

with a closely apposed base B (the oxidation of Y_ZH yields $Y_Z^{\bullet}\cdots H^+\cdots B$). (Such a proton rocking has originally been proposed by Babcock et al. (22) to account for the EPR signal of Y_D^{ox} which indicates a neutral (i.e. deprotonated) radical.) (2) with the absence of the hydroxyl proton (e.g. the presence of a tyrosinate) in the reduced state (the oxidation of Y_Z^- is supposed to yield Y_Z^{\bullet}).

That Y_Z in its reduced state may be a tyrosinate has also been speculated on the basis of a recent study of tyrosine oxidation in vitro by pulse radiolysis (57). The spectra in our work argue against both, a proton rocking motion, analogous to the Y_D case, and a free tyrosinate, Tyr^- , in the reduced state. They are better compatible with the presence of a hydrogen-bonded tyrosinate ($Tyr^{(-)}\cdots H^{(+)}\cdots B$) with spectral properties that differ from both, Tyr^- and $TyrH$. Such a structure has been reported to exist in several proteins and artificial systems. It is intermediate between (1) and (2): The proton within the hydrogen bond is shifted toward the base B already in the reduced state. It is plausible that the rate of electron transfer in such a system is independent of the very slight proton movements (in contrast to Y_D where the proton rocking slows the reaction). The hydrogen-bonded tyrosinate $Y_Z^{(-)}\cdots H^{(+)}\cdots B$ is oxidized to the hydrogen-bonded radical $Y_Z^{\bullet}\cdots H^+\cdots B$ with the positive charge of the proton trapped between Y_Z and B. The different spectral properties of Y_Z in Mn-depleted centers when going from alkaline to acid pH may indicate the abolishing (or weakening) of its hydrogen bonds, both in the reduced and oxidized state. During the oxidation of Y_ZH to $Y_Z^{\bullet} + H^+$ the phenolic proton is then released into the aqueous bulk.

The presence of a hydrogen-bonded tyrosinate requires the presence of residues next to Y_Z that are stronger bases than Y_Z itself. From mutagenesis (88–91) and modeling studies (14, 92) of PSII it has been proposed that D1His190 is likely one hydrogen bond acceptor of Y_Z . There are further hydrogen-bonding amino acid residues in close proximity to Y_Z , namely Asp170 and Glu189 (81, 98). On the D2 subunit D2His190 has been established as a hydrogen bond acceptor to Y_D (93–97), with counterparts to the latter two residues being missing. The mutation of both residues to nonbonding ones largely or fully suppresses oxygen evolution (88, 99–102). Interestingly, on the M-subunit of the reaction center of *Rps. viridis* the homologous residues (MTyr191, MHis162, MArg190, and MGlu171) seem to form a hydrogen-bonded cluster (see Chart 1A). The distances between these residues (Chart 1A) favor three hydrogen bonds: Two between the hydroxyl function of Tyr191 to His162 and Glu171 and one between His162 and Glu171 (103). We speculate that a similar hydrogen-bonding network (cluster) is conserved in PSII. Scheme 1B shows a hypothetical structure based on the one shown in Chart 1A where the residues of the bacterial RC are substituted for their homologues from PSII *without changing the backbone coordinates*. Y_Z (Tyr161) may be bonded to His190 and (via a water bridge) also to some other residue (Asp170?) (two hydrogen bonds to the hydroxyl function of Y_Z have already been observed by ENDOR under certain conditions (G. Babcock, personal communication)). His190, in turn, may be additionally H-bonded to Glu189 (Scheme 1B). That the exchange of Glu189 against Gln preserves oxygen evolution which is abolished by a *shorter* Asp argues in favor of this suggestion ((91), see also ref 19). A hydrogen bonding network as shown

Chart 1: Putative Hydrogen-Bonded Clusters in *Rps. viridis* and PSII^a



^aKey: (A) Arrangement of four amino acid residues of the M-subunit of *Rps. viridis* (1). The presumed hydrogen bonds are depicted as broken lines. (B) Hypothetical arrangement of the four amino acid residues of the D1 subunit of PSII in the positions homologous to the bacterial RC. The arrangement has been obtained by replacing the residues in the M-subunit of *Rps. viridis* by the respective residues in PSII without changing the backbone coordinates and without further optimization of the structure. The putative hydrogen bonds are again shown as broken lines. A further hydrogen bond between Tyr161 and Asp170 is conceivable if one allows for minor structural rearrangements.

in Scheme 1B is expected to lower the pK of Y_Z and to increase the one of His190. More specifically, we suggest that a strong H-bonding between His190 and Glu189 favors the formation of a hydrogen-bonded tyrosinate. Our view gains support from the recent observation of tyrosine oxidation only in the M-subunit of the bacterial reaction center where the potential of the primary donor has been elevated to ~ 850 mV by genetical engineering and tyrosine residues have been introduced in both the L and M subunits (J. Allen, personal communication at the XIth Congress on Photosynthesis, Budapest). Thus, the M-subunit may model the vicinity of Y_Z on the D1 protein of PSII better than the corresponding part of the L-subunit which has been used in previous model attempts (14, 98).

The oxidation of Y_Z is not limited by the proton transfer within the hydrogen-bonded network. If, on the other hand, the acid–base network is already protonated, as at acid pH in Mn-depleted centers, the phenolic proton has to be deposited into the aqueous bulk before electron-transfer proceeds (ref 37 and this work). According to Scheme 1B it is likely that the apparent pK of 7 in Mn-depleted centers belongs to the $Y_ZH\cdots His190\cdots Glu189$ network. A similar “tuning” of the pK in a hydrogen-bonded network is known from trypsin. An apparent pK of 7 has been observed in the catalytic triade of this protease. A serine residue (pK about 13 in water) donates its hydroxyl proton to a histidine residue.

Histidine is "activated" as a proton acceptor by a further, strong hydrogen bond with an aspartic acid (104, 105).

According to our UV difference spectra it is likely that hydrogen bonding both of Y_ZH and Y_Z^* is lost at acidic pH in Mn-depleted centers. The reason may be the destruction of the hydrogen bonding net by the insertion of an additional proton which causes structural changes in the system. This suggestion is in line with the increased recombination rate between Y_Z^{ox} and Q_A^- at acidic pH (60, 106) which indicates an increase of the midpoint potential of Y_Z . It is further in line with the observation that the ENDOR spectrum of Y_Z^{ox} at pH 5.5 in Mn-depleted centers strongly differs from the one at pH 7.5. In the spectrum at pH 5.5 the hyperfine interaction of the OH proton was no longer detected (107, 108). Interestingly, a similar ENDOR spectrum that was observed in Mn-depleted centers at pH 5.5 was also observed in Ca^{2+} -depleted ones over a wider pH range (107, 108). It was with the latter preparation that the short 5 Å distance between Y_Z and, presumably, the Mn-cluster has been claimed (23). Thus, in the Ca^{2+} -depleted system the environment of Y_Z may be *structurally* rather different relative to the native system where the distance between Y_Z and the various components of the Mn cluster has been estimated as 8–20 Å (30, 109, 117). This suggestion is in line with the observed strong retardation of electron transfer between Y_Z and P_{680}^+ in Ca-depleted PSII (29, 83, 110). On the contrary, in Cl^- -depleted centers where electron transfer from Y_Z to P_{680}^+ occurs as fast as in controls, i.e., in nanoseconds (8), the difference spectrum $Y_Z^{ox} - Y_Z$ (8, 111) is similar to the one measured in oxygen-evolving centers in the whole spectral region. This indicates a more similar environment of Y_Z in oxygen-evolving and Cl^- -depleted centers.

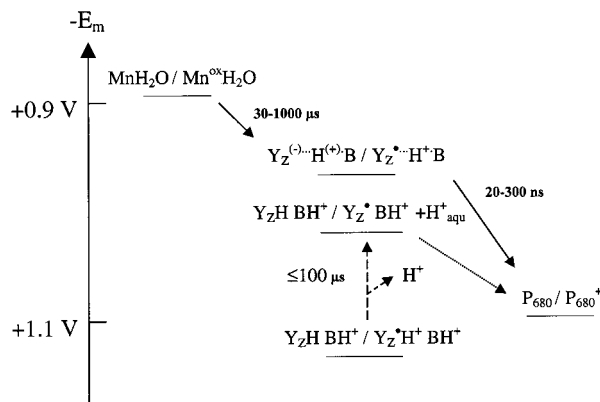
In our previous work (37) we have shown that in Mn-depleted centers and at low pH the phenolic proton from tyrosine is released into the medium. Only under these conditions (low pH, Mn-depleted centers) the Y_Z^{ox} site appears to be neutral. Under all other conditions the proton is not released and the site is positively upcharged and thus inappropriate to accept a hydrogen atom from water as suggested in refs 18–20 and 112–114. The structural analogy with the catalytic triade of serine proteases might explain why, in the latter case, the proton is trapped in the protein.

The positive charge of the trapped proton may elevate the redox potential of Mn relative to the one of bound water by up to 100 mV. It is likely that the state S_4 is equivalent to $4Mn^{2ox}X^{ox}Y_Z \cdots H^+ \cdot B$ (33, 123). As discussed elsewhere (33, 37, 123), the positive charge on $Y_Z \cdots H^+ \cdot B$ may then provide the final overpotential that shifts the equilibrium between bound water and peroxide toward the latter thereby initiating the reaction cascade of water oxidation upon transition $S_4 \rightarrow S_0$.

CONCLUSIONS

The following interpretation may help to understand hitherto seemingly contradictory observations: Our data imply that, in oxygen-evolving PSII centers, the redox active tyrosine, Y_Z , is present as a hydrogen-bonded tyrosinate, $Y_Z(-) \cdots H^{(+)} \cdot B$, with spectral properties intermediate between free tyrosine, TyrH, and free tyrosinate, Tyr^- . B is possibly D1His190 in hydrogen-bonding interaction with other amino

Scheme 1: Relative Midpoint Potentials of the Redox Cofactors at the Oxidizing Side of PSII^a



^a The couple P_{680}^+/P_{680} is placed at about 1.1 V (78). The cluster of four Mn atoms and two water molecules is symbolized as Mn/H₂O. Its potential is by less than 300 mV lower than the one of P_{680} . Electron transfer in oxygen-evolving PSII is depicted by solid arrows. Y_Z is a hydrogen-bonded tyrosinate in the reduced state and still hydrogen bonded when oxidized. Its midpoint potential is intercalated between Mn/H₂O and P_{680} . Electron transfer in Mn-depleted centers at acid pH is shown by a dotted arrow. The midpoint potential of the Y_Z radical with the proton still on the phenol is too positive to reduce P_{680}^+ . It proceeds only through the electrostatic relaxation by the release of the proton into the bulk (dashed arrow). The reaction rate is comparable with the one of charge recombination between P_{680}^+ and Q_A^- . The midpoint potential of Y_Z in Mn-depleted centers at acid pH may be somewhat higher than at alkaline pH due to the additional proton in the Y_Z/B system (B represents for the amino acids in the hydrogen-bonded network).

acids. Upon the oxidation of Y_Z by P_{680}^+ in nanoseconds the phenolic proton stays within the hydrogen-bonded network. The charge is more delocalized, but it resides still in close vicinity of Y_Z . Thereby $Y_Z \cdots H^+ \cdot B$ appears as a neutral radical (EPR), but the whole entity is positively upcharged causing transient electrochromism.

In the intact, oxygen-evolving PSII we propose a hydrogen-bonded network between Y_Z and a series of amino acids (coined B), conceivably His190, Glu189, and Asp170 (Chart 1B). The hydrogen bond between Y_Z and B allows for the rapid reduction of P_{680}^+ in nanoseconds. It is not rate limited by proton transfer. Moreover, it lowers the redox potential of Y_Z compared to the one of the respective nonbonded species, which is too positive to reduce P_{680}^+ . This is detailed in Scheme 1. Because the more negative midpoint potential of the hydrogen-bonded system is intercalated between the ones of P_{680} and the Mn–water cluster, Y_Z can serve both as a reductant to P_{680}^+ and as an oxidant to the Mn–water cluster. When the hydrogen bonded net is broken, $Y_Z \cdot H^+$ is too positive to reduce P_{680}^+ , unless the phenolic proton is released into the aqueous bulk (in $\leq 100 \mu s$; see dashed arrow in Scheme 1). In this case the rate of the electron transfer between Y_Z and P_{680} is essentially the same as the rate of the proton transfer. The rate of the reaction then reflects the shift of the thermodynamical redox equilibrium between Y_Z and P_{680} as a consequence of the deprotonation, rather than the kinetic properties of the (supposedly much more rapid) electron-transfer itself (dotted arrow).

ACKNOWLEDGMENT

The authors appreciate stimulating discussions with Dr. D. Cherepanov, Monika Hundelt, and Ralf Ahlbrink. We

thank Dr. S. Engelbrecht for his help with the structural modeling and Hella Kenneweg for excellent technical assistance.

REFERENCES

- Michel, H., and Deisenhofer, J. (1988) *Biochemistry* 27, No. 1, 1–7.
- Renger, G. (1997) *Physiol. Plant* 100, 828–841.
- Debus, R. J., Barry, B. A., Babcock, G. T., and McIntosh, L. (1988) *Proc. Natl. Acad. Sci. U.S.A.* 85, 427–430.
- Metz, J. G., Nixon, P. J., Rögner, M., Brudvig, G. W., and Diner, B. A. (1989) *Biochemistry* 28, 6960–6969.
- Yachandra, V. K., Sauer, K., and Klein, M. P. (1996) *Chem. Rev.* 96, 2927–2950.
- Penner-Hahn, J. E. (1998) *Struct. Bonding* 90, 1–36.
- Boussac, A., and Rutherford, A. W. (1994) *J. Biol. Chem.* 269, 12462–12467.
- Haumann, M., Drevstedt, W., Hundelt, M., and Junge, W. (1996) *Biochim. Biophys. Acta* 1273, 237–250.
- Hundelt, M., Haumann, M., and Junge, W. (1997) *Biochim. Biophys. Acta* 1321, 47–60.
- Lindberg, K., and Andreasson, L. E. (1996) *Biochemistry* 35, 14259–14267.
- Ono, T., and Inoue, I. (1988) *FEBS Lett.* 227, No. 2, 147–152.
- Shen, J. R., Satoh, K., and Katoh, S. (1988) *Biochim. Biophys. Acta* 936, 386–394.
- van Vliet, P., and Rutherford, A. W. (1996) *Biochemistry* 35, 1829–1839.
- Styring, S., Davidsson, L., Tommos, C., Vermaas, W. F. J., Vass, I., and Svensson, B. (1993) *Photosynthetica* 28, 225–241.
- Mulkijanian, A. Y., Cherepanov, D. A., Haumann, M., and Junge, W. (1996) *Biochemistry* 35, 3093–3107.
- Haumann, M., Mulkijanian, A. Y., and Junge, W. (1997) *Biochemistry* 36, 9304–9315.
- Pokorny, A., Wulf, K., and Trissl, H. W. (1994) *Biochim. Biophys. Acta* 1184, 65–70.
- Babcock, G. T. (1995) in *Photosynthesis: From Light to Biosphere. Vol. 2* (Mathis, P., Ed.) pp 209–215, Kluwer Academic Publishers, Dordrecht, The Netherlands.
- Hoganson, C. W., and Babcock, G. T. (1997) *Science* 277, 1953–1956.
- Babcock, G. T., Espe, M., Hoganson, C., Lydakis-Simantiris, N., McCracken, J., Shi, W., Styring, S., Tommos, C., and Warncke, K. (1997) *Acta Chem. Scand.* 51, 533–540.
- Nugent, J. H. A. (1996) *Eur. J. Biochem.* 237, 519–531.
- Babcock, G. T., Barry, B. A., Debus, R. J., Hoganson, C. W., Atamian, M., McIntosh, L., Sithole, U., and Yocum, C. F. (1989) *Biochemistry* 28, 9557–9565.
- Gilchrist, M. L., Ball, J. A., Randall, D. W., and Britt, R. D. (1995) *Proc. Natl. Acad. Sci. U.S.A.* 92, 9545–9549.
- Peloquin, J. M., Campbell, K. A., and Britt, R. D. (1998) *J. Am. Chem. Soc.*, in press.
- Renger, G., and Völker, M. (1982) *FEBS Lett.* 149, 203–207.
- Förster, V., and Junge, W. (1984) in *Advances in Photosynthetic Research* (Sybesma, C., Ed.) pp 305–309, Martinus Nijhoff/Dr W. Junk, The Hague/Boston/Lancaster.
- Haumann, M., and Junge, W. (1994) *Biochemistry* 33, 864–872.
- Bögershausen, O., and Junge, W. (1995) *Biochim. Biophys. Acta* 1230, 177–185.
- Boussac, A., Setif, P., and Rutherford, A. W. (1992) *Biochemistry* 31, 1224–1234.
- Kodera, Y., Hara, H., Astashkin, A. V., Kawamori, A., and Ono, T. (1995) *Biochim. Biophys. Acta* 1232, 43–51.
- Mino, H., Kawamori, A., Matsukawa, T., and Ono, T. A. (1998) *Biochemistry* 37, 2794–2799.
- Smith, P. J., and Pace, R. J. (1996) *Biochim. Biophys. Acta* 1275, 213–220.
- Haumann, M., Bögershausen, O., Cherepanov, D. A., Ahlbrink, R., and Junge, W. (1997) *Photosynth. Res.* 51, 193–208.
- Haumann, M., and Junge, W. (1996) in *Oxygenic Photosynthesis—The Light Reactions* (Ort, D., and Yocum, C. F., Eds.) pp 165–192, Kluwer Academic Publishers, Dordrecht, The Netherlands.
- Karge, M., Irrgang, K. D., Sellin, S., Feinaeugle, R., Liu, B., Eckert, H. J., Eichler, H. J., and Renger, G. (1996) *FEBS Lett.* 378, 140–144.
- Schilstra, M. J., Rappaport, F., Nugent, J. H. A., Barnett, C. J., and Klug, D. R. (1998) *Biochemistry* 37, 3974–3981.
- Ahlbrink, R., Haumann, M., Cherepanov, D., Bögershausen, O., Mulkijanian, A., and Junge, W. (1998) *Biochemistry* 37, 1131–1142.
- Renger, G., Eckert, H. J., Hagemann, R., Hanssum, B., Koike, H., and Wacker, U. (1989) in *Photosynthesis: Molecular Biology and Bioenergetics* (Singhal, G. S., Barber, J., Dilley, R. A., Govindjee, Haselkorn, R., and Mohanty, P., Eds.) pp 357–371, Narosa Publ. House, New Delhi.
- Lavergne, J. (1989) *Photochem. Photobiol.* 50, 235–241.
- Rappaport, F., Blanchard-Desce, M., and Lavergne, J. (1994) *Biochim. Biophys. Acta* 1184, 178–192.
- van Leeuwen, P. J., Nieveen, M. C., van de Meent, E. J., Dekker, J. P., and van Gorkom, H. J. (1991) *Photosynth. Res.* 28, 149–153.
- Renger, G. (1979) *Biochim. Biophys. Acta* 547, 103–116.
- Cheniae, G. M., and Martin, I. F. (1978) *Biochim. Biophys. Acta* 502, 321–344.
- Cole, J., Boska, M., Blough, N. V., and Sauer, K. (1986) *Biochim. Biophys. Acta* 848, 41–47.
- Junge, W. (1976) in *Chemistry and Biochemistry of Plant Pigments* (Goodwin, T. W., Ed.) pp 233–333, Academic Press, London, New York, San Francisco, CA.
- Lavergne, J. (1982) *Biochim. Biophys. Acta* 679, 12–18.
- Dekker, J. P., van Gorkom, H. J., Brok, M., and Ouwehand, L. (1984) *Biochim. Biophys. Acta* 764, 301–309.
- Diner, B. A., and de Vitry, C. (1984) in *Advances in Photosynthesis* (Sybesma, C., Ed.) pp 407–411, Martinus Nijhoff/Dr W. Junk, The Hague/Boston/Lancaster.
- Dekker, J. P., van Gorkom, H. J., Wensink, J., and Ouwehand, L. (1984) *Biochim. Biophys. Acta* 767, 1–9.
- Gerken, S., Dekker, J. P., Schlopper, E., and Witt, H. T. (1989) *Biochim. Biophys. Acta* 977, 52–61.
- van Leeuwen, P. J., Heimann, C., and van Gorkom, H. J. (1993) *Photosynth. Res.* 38, 323–330.
- Bögershausen, O., and Junge, W. (1995) in *Photosynthesis: from Light to Biosphere* (Mathis, P., Ed.) pp 263–266, Kluwer Academic Publishers, Dordrecht, The Netherlands.
- Bögershausen, O., Haumann, M., and Junge, W. (1996) *Ber. Bunsen-Ges. Phys. Chem.* 100, 1987–1992.
- Hillmann, B., Brettel, K., van Mieghem, F. J. E., Kamlowski, A., Rutherford, A. W., and Schlopper, E. (1995) *Biochemistry* 34, 4814–4827.
- Dekker, J. P. (1985) Thesis, University of Leiden.
- Diner, B. A., Tang, X. S., Zheng, M., Dismukes, G. C., Force, D. A., Randall, D. W., and Britt, R. D. (1995) in *Photosynthesis: From Light to Biosphere. Vol. 2* (Mathis, P., Ed.) pp 229–234, Kluwer Academic Publishers, Dordrecht, The Netherlands.
- Candeias, L. P., Turconi, S., and Nugent, J. H. A. (1998) *Biochim. Biophys. Acta* 1363, 1–5.
- Bent, D. V., and Hayon, E. (1975) *J. Am. Chem. Soc.* 97, 2599–2606.
- Lavergne, J. (1984) *FEBS Lett.* 173, No. 1, 9–14.
- Rappaport, F., and Lavergne, J. (1997) *Biochemistry* 36, 15294–15302.
- Land, E. J., Porter, G., and Strachan, E. (1961) *Trans. Faraday Soc.* 57, 1885–1893.
- Lakowicz, J. R. (1986) *Principles of Fluorescence Spectroscopy* Plenum Press, New York.
- Pundak, S., and Roche, R. S. (1984) *Biochemistry* 23 (7), 1549–1555.
- Szabo, A. G., Lynn, K. R., Krajcarski, D. T., and Rayner, D. M. (1978) *FEBS Lett.* 94 (2), 249–252.
- Jordano, J., Barbero, J. L., Montero, F., and Franco, L. (1983) *J. Biol. Chem.* 258 (1), 315–320.

66. Mach, H., Middaugh, C. R., and Lewis, R. V. (1992) *Anal. Biochem.* 200, 74–80.
67. Turner, R. J., and Moore, G. J. (1992) *Biochim. Biophys. Acta* 1117, 265–270.
68. Bicknell-Brown, E., Lim, B. T., and Kimura, T. (1981) *Biochem. Biophys. Res. Commun.* 101 (1), 298–305.
69. Dobson, G., and Grossweiner, L. I. (1965) *Trans. Faraday Soc.* 61, 708–714.
70. Land, E. J., and Ebert, M. (1967) *Trans. Faraday Soc.* 63, 1181–1190.
71. Tang, X. S., Zheng, M., Chisholm, D. A., Dismukes, G. C., and Diner, B. A. (1996) *Biochemistry* 35, 1475–1484.
72. Un, S., Tang, X. S., and Diner, B. A. (1996) *Biochemistry* 35, 679–684.
73. Force, D. A., Randall, D. W., Britt, R. D., Tang, X. S., and Diner, B. A. (1995) *J. Am. Chem. Soc.* 117, 12643–12644.
74. Mino, H., Satoh, J., Kawamori, A., Toriyama, K., and Zimmermann, J. L. (1993) *Biochim. Biophys. Acta* 1144, 426–433.
75. Tommos, C., Davidsson, L., Svensson, B., Madsen, C., Vermaas, W. F. J., and Styring, S. (1993) *Biochemistry* 32, 5436–5441.
76. Farrar, C. T., Gerfen, G. J., Griffin, R. G., Force, D. A., and Britt, R. D. (1997) *J. Phys. Chem. B* 101, 6634–6641.
77. Marcus, R. A., and Sutin, N. (1985) *Biochim. Biophys. Acta* 811, 265–322.
78. Klimov, V. V., Allakhverdiev, S. I., Demeter, S., and Krasnovskii, A. A. (1979) *Dokl. Akad. Nauk SSSR* 249, 227–230.
79. Hoganson, C. W., and Babcock, G. T. (1989) *Biochemistry* 28, 1448–1454.
80. Rutherford, A. W. (1986) *Biochem. Soc. Trans.* 14, 15–17.
81. Svensson, B., Etchebest, C., Tuffery, P., van Kan, P., Smith, J., and Styring, S. (1996) *Biochemistry* 35, 14486–14502.
82. Moser, C. C., Keske, J. M., Warncke, K., Farid, R. S., and Dutton, P. L. (1992) *Nature* 355, 796–802.
83. Renger, G., Eckert, H. J., and Völker, M. (1989) *Photosynth. Res.* 22, 247–256.
84. Brettel, K., Schlodder, E., and Witt, H. T. (1984) *Biochim. Biophys. Acta* 766, 403–415.
85. van Leeuwen, P. J., Heimann, C., Kleinherenbrink, F. A. M., and van Gorkom, H. J. (1992) in *Research in Photosynthesis* (Murata, N., Ed.) pp 341–344, Kluwer Academic Publishers, Dordrecht, The Netherlands.
86. Lukins, P. B., Post, A., Walker, P. J., and Larkum, A. W. D. (1996) *Photosynth. Res.* 49, 209–221.
87. Krishtalik, L. I. (1995) *Biochim. Biophys. Acta* 1228, 58–66.
88. Chu, H. A., Nguyen, A. P., and Debus, R. J. (1995) *Biochemistry* 34, 5859–5882.
89. Hays, A. M., Vassiliev, I. R., Golbeck, J. H., and Debus, R. J. (1998) *Biochemistry*, submitted for publication.
90. Roffey, R. A., van Wijk, K. J., Sayre, R. T., and Styring, S. (1994) *J. Biol. Chem.* 269, 5115–5121.
91. Chu, H. A., Nguyen, A. P., and Debus, R. J. (1995) *Biochemistry* 34, 5839–5858.
92. Ruffle, S. V., and Nugent, J. H. A. (1992) in *Research in Photosynthesis. Vol. 2* (Murata, N. Ed.) pp 191–194, Kluwer Academic Publishers, Dordrecht, The Netherlands.
93. Campbell, K. A., Peloquin, J. M., Diner, B. A., Tang, X.-S., Chisholm, D. A., and Britt, R. D. (1997) *J. Am. Chem. Soc.* 119, 4787–4788.
94. Kim, S., Liang, J., and Barry, B. A. (1997) *Proc. Natl. Acad. Sci. U.S.A.* 94, 14406–14411.
95. MacDonald, G. M., Bixby, K. A., and Barry, B. A. (1993) *Proc. Natl. Acad. Sci. U.S.A.* 90, 11024–11028.
96. Kim, S., and Barry, B. A. (1998) *Biophys. J.* 74, 2588–2600.
97. Hienerwadel, R., Boussac, A., Breton, J., Diner, B. A., and Berthomieu, C. (1997) *Biochemistry* 36, 14712–14723.
98. Ruffle, S. V., Donnelly, D., Blundell, T. L., and Nugent, J. H. A. (1992) *Photosynth. Res.* 34, 287–300.
99. Diner, B. A., and Nixon, P. J. (1992) *Biochim. Biophys. Acta* 1101, 134–138.
100. Nixon, P. J., and Diner, B. A. (1992) *Biochemistry* 31, 942–948.
101. Nixon, P. J., and Diner, B. A. (1991) *Photochem. Photobiol.* 53, 71–78.
102. Vermaas, W. (1993) *Annu. Rev. Plant Physiol. Plant Mol. Biol.* 44, 457–481.
103. Deisenhofer, J., Sinning, I., and Michel, H. (1995) *J. Mol. Biol.* 246, 429–457.
104. Smith, S. O., Farr-Jones, S., Griffin, R. G., and Bachovchin, W. W. (1989) *Science* 244, 961–964.
105. Cleland, W. W., and Kreevoy, M. M. (1994) *Science* 264, 1887–1890.
106. Shigemori, K., Mino, H., and Kawamori, A. (1997) *Plant Cell Physiol.* 38, 1007–1011.
107. Mino, H., Astashkin, A. V., Kawamori, A., Ono, T., and Inoue, Y. (1995) in *Photosynthesis: From Light to Biosphere. Vol. 1* (Mathis, P., Ed.) pp 559–562, Kluwer Academic Publishers, Dordrecht, The Netherlands.
108. Mino, H., Astashkin, A. V., and Kawamori, A. (1997) *Spectrochim. Acta* 53A, 1465–1483.
109. Szalai, V. A., Kühne, H., Lakshmi, K. V., Eaton, G. R., Eaton, S. S., and Brudvig, G. W. (1998) *Biophys. J.* 74 (2), 75.
110. Koike, H., Kashino, Y., Inoue, Y., and Satoh, K. (1992) in *Research in Photosynthesis. Vol. 2* (Murata, N. Ed.) pp 369–372, Kluwer Academic Publishers, Dordrecht, The Netherlands.
111. Wincencjusz, H., van Gorkom, H. J., and Yocum, C. F. (1997) *Biochemistry* 36, 3663–3670.
112. Britt, R. D. (1996) in *Oxygenic Photosynthesis: The Light Reactions* (Ort, D., and Yocum, C. F., Eds.) pp 137–164, Kluwer Academic Publishers, Dordrecht, The Netherlands.
113. Tommos, C., and Babcock, G. T. (1998) *Acc. Chem. Res.* 31, 18–25.
114. Tommos, C., Hoganson, C. W., Di Valentin, M., Lydakis-Simantiris, N., Dorlet, P., Westphal, K., Chu, H. A., McCracken, J., and Babcock, G. T. (1998) *Curr. Opin. Chem. Biol.*, in press.
115. Renger, G., Eckert, H. J., and Buchwald, H. E. (1978) *FEBS Lett.* 90 (1), 10–14.
116. Schlodder, E., Brettel, K., Schatz, G. H., and Witt, H. T. (1984) *Biochim. Biophys. Acta* 765, 178–185.
117. Hara, H., Kawamori, A., Astashkin, A. V., and Ono, T. (1996) *Biochim. Biophys. Acta* 1276, 140–146.
118. Conjeaud, H., and Mathis, P. (1980) *Biochim. Biophys. Acta* 590, 353–359.
119. Haumann, M., Ahlbrink, R., and Junge, W. (1998) *Proc. XIth Congr. Photosynth., Budapest*, in press.
120. Schatz, G. H., and van Gorkom, H. J. (1985) *Biochim. Biophys. Acta* 810, 283–294.
121. Gerken, S., Brettel, K., Schlodder, E., and Witt, H. T. (1988) *FEBS Lett.* 237, 69–75.
122. Haumann, M., Hundelt, M., Jahns, P., Chroni, S., Bögershausen, O., Ghanotakis, D., and Junge, W. (1997) *FEBS Lett.* 410, 243–248.
123. Karge, M., Irrgang, K.-D., and Renger, G. (1997) *Biochemistry* 36 (29), 8904–8913.
124. Renger, G., Christen, G., Karge, M., Eckert, H.-J., and Irrgang, K.-D. (1998) *J. Biol. Inorg. Chem.*, in press.